THE ROCKETDYNE MULTIFUNCTION TESTER PART I: TEST METHOD[1]

B.T. MURPHY
JOSEPH K. SCHARRER
ROBERT F. SUTTON
ROCKWELL INTERNATIONAL
CANOGA PARK, CALIFORNIA 91304

ABSTRACT

The Rocketdyne Multifunction Tester is a general purpose test apparatus which utilizes axial and radial magnetic bearings as shaft excitation devices. The tester is modular in design so that different seal and bearing packages can be tested on the same test stand. The tester will be used for rotordynamic coefficient extraction, as well as life and fluid/material compatibility evaluations. Use of a magnetic bearing as a shaft excitation device opens up many possibilities for shaft excitation and rotordynamic coefficient extraction. In addition to describing the basic apparatus, this paper will discuss some of the excitation and extraction methods considered, and detail the chosen method. Some of the excitation methods to be discussed include random, aperiodic, harmonic, impulse and chirp.

INTRODUCTION

Recent trends in the design of high-performance turbomachinery for advanced pump-fed liquid rocket engines have moved away from rolling element bearings in favor of fluid film elements. The potential payoffs are longer life, higher admissible DN values, and more control over turbopump rotordynamics. Hydrostatic bearings and annular seals appear most promising. In effort to support the new designs, Rocketdyne has designed, and is currently fabricating, a multifunction bearing and seal tester. The goals are to measure accurate rotordynamic coefficients, conduct durability tests, and evaluate different materials, all in an environment simulating real cryogenic turbopump operating conditions. Measurement of rotordynamic coefficients is accomplished via the use of a radial magnetic bearing as a shaft motion exciter. Test bearing (or seal) reaction load is measured in the support structure. The versatility of the magnetic bearing as an exciter is the key feature of this tester.

The purpose of this article is to describe the basic methods which will be used to excite the shaft, acquire the data, and reduce the data. All three of these tasks are to be performed by a single computer. The tester is designed to run the test bearing (or seal) at a constant operating point, and use the magnetic bearing to excite the shaft in a manner suitable to permit identification of the bearing's (or seal's) complex impedance functions.

[1]This work was partially supported by United States Air Force contract F04611-86-C-0103

The impedance functions then yield the desired rotordynamic stiffness, damping and mass coefficients.

The application of a magnetic bearing in this manner is novel, thus there is a degree of uncertainty as to how well it will function, and what the optimum input signal will be (i.e., random, aperiodic, harmonic, swept sine, impulse, step, chirp, etc.). The versatility of having a completely arbitrary waveform generator is, therefore, most important. Also, it is desirable that the input signal delivered to the magnetic bearing be adaptive so that optimum signal to noise ratios can be achieved.

The key constraint in this test program is length of test time. Many of the tests are limited to about 5 minutes each by virtue of the blow down facility being used. In all, approximately 35 such tests are currently planned. These 35 tests are divided among different seals, different bearings, and different working fluids. Each 5 minute test must encompass a multitude of operating points (combinations of shaft speed, pressure drop, inlet swirls, eccentricities, etc.). Presently, only about 20 seconds of test time are being allotted to each operating point for measurement of rotordynamic coefficients. The chosen input signal must make optimum use of this limited amount of time.

DESCRIPTION OF APPARATUS

The multifunction tester, configured with an annular seal, is depicted in figure 1. The tester consists of the basic tester and a module containing the test article. The basic tester rotor is supported on one end by a duplex ball bearing and on the other by the magnetic bearing. The module contains the test article only. When assembled, the main rotor supports are the duplex ball bearing and the test article, use of the magnetic bearing as a support is optional as discussed by Hawkins, et al. (ref. 1).

The main function of the magnetic bearing is to generate asynchronous motion of the rotor at the test article. The reaction force at the test article is measured using a calibrated cylindrical spring called a flexmount. The deflection of the flexmount under load is measured using four Bently REBAM proximity probes. The acceleration of the flexmount is measured in two orthogonal directions using PCB accelerometers to allow for correction of stator inertia. The motion of the rotor at the test article is measured using Bently proximity probes.

The initial test plan calls for testing of a 152.4 mm (6.0 inch) diameter annular seal, a 88.9 mm (3.5 inch) diameter hydrostatic bearing, and a 57 mm (2.24 inch) ball bearing in LN2 and actual cryogenic propellants. The annular seal will be tested at three different values of inlet swirl. The tester will operate at speeds up to 24,000 cpm and supply pressures to 172.4 Bar (2500 psi), for this test series. The maximum tester design speed is 30,000 cpm. The geometries for the test articles will reflect those envisioned for production rocket engine turbomachinery. This requires radial clearances in the range of 0.076-0.127 mm (0.003-0.005 inches), whereas all test results to date are for radial clearances in the range 0.254-0.508 mm (0.010-0.020 inches) and at lower shaft speeds.

FUNDAMENTALS OF ROTORDYNAMIC COEFFICIENT MEASUREMENT

The standard relationship between bearing displacements and forces in the time domain is expressed as follows:

$$[M]\ddot{q} + [C]\dot{q} + [K]q = F \tag{1}$$

Rotors operating at steady state execute motions which are strongly periodic (i.e, harmonic). This lends itself to a frequency domain representation. Also, from a test point of view, it is more convenient to work in the frequency domain. Thus, transforming equation (1) to the frequency domain and employing complex notation (equivalent to amplitude and phase) results in:

$$\begin{bmatrix} (K_{xx} + iC_{xx}\omega - M_{xx}\omega^2) & (K_{xy} + iC_{xy}\omega - M_{xy}\omega^2) \\ (K_{yx} + iC_{yx}\omega - M_{yx}\omega^2) & (K_{yy} + iC_{yy}\omega - M_{yy}\omega^2) \end{bmatrix} \begin{Bmatrix} \bar{x} \\ \bar{y} \end{Bmatrix} = \begin{Bmatrix} \bar{F}_x \\ \bar{F}_y \end{Bmatrix} \tag{2a}$$

or

$$\begin{bmatrix} Z_{xx} & Z_{xy} \\ Z_{yx} & Z_{yy} \end{bmatrix} \begin{Bmatrix} \bar{x} \\ \bar{y} \end{Bmatrix} = \begin{Bmatrix} \bar{F}_x \\ \bar{F}_y \end{Bmatrix} \tag{2b}$$

In the usual sense, the physical displacement in the x direction is the real part of the complex expression $\bar{x}e^{i\omega t}$ and similarly, for y, F_x and F_y. The complex impedances, Z, come directly from measurements of $\bar{x}$, $\bar{y}$, $\bar{F}_x$ and $\bar{F}_y$, all presumably as functions of frequency. The displacements x and y are usually obtained easily with non-contacting displacement probes. The forces F_x and F_y are more difficult, and may be measured directly with special load cells, or inferred indirectly from some other known quantities such as pressure distribution, a hammer impulse, intentional unbalance, or the snap of a suddenly released static load. Once the displacements and forces are obtained as functions of frequency, the exact procedure for obtaining the impedances Z, and in turn, the rotordynamic coefficients, depends on how the displacements and forces were generated (i.e., the overall test approach). The reduction procedures for several test approaches considered for the multifunction tester will now be described.

Single Circular Orbits - A very natural approach is to use the magnetic bearing to impart a circular whirl orbit to the rotor, and vary its frequency over the frequency range of interest (rotor speed held constant). In this case $\bar{y} = \bar{x}e^{-i\frac{\pi}{2}}$ (counterclockwise orbit) at each value of frequency giving the following:

$$\begin{aligned} Z_{xx} + Z_{xy}e^{-i\frac{\pi}{2}} &= \frac{\bar{F}_x}{\bar{x}} = K_{xx} + C_{xy}\omega - M_{xx}\omega^2 - i(K_{xy} - C_{xx}\omega - M_{xy}\omega^2) \\ Z_{yx} + Z_{yy}e^{-i\frac{\pi}{2}} &= \frac{\bar{F}_y}{\bar{x}} = K_{yx} + C_{yy}\omega - M_{yx}\omega^2 - i(K_{yy} - C_{yx}\omega - M_{yy}\omega^2) \end{aligned} \tag{3}$$

The $\bar{x}$, $\bar{F}_x$ and $\bar{F}_y$ data obtained for a single circular orbit are not sufficient to completely determine all 4 complex Z's. However, the special shape of the orbit does permit

their partial determination by grouping of their real and imaginary components as shown. The 4 components (real and imaginary parts of $\bar{F}_x/\bar{x}$ and $\bar{F}_y/\bar{x}$) can be plotted versus frequency, and curve fits yield the 12 desired rotordynamic coefficients. Note that all 12 coefficients must be real which precludes the detection of mechanisms like hysteretic damping. Note also that there is no benefit to assuming skew symmetric stiffness, damping and mass matrices. The only information obtained as to the adequacy of the assumed KCM model is via digression from a pure quadratic. This test approach is used by Adams, et al. (ref. 2).

Dual Circular Orbits - The magnetic bearing is capable of producing either forward or backward circular whirl orbits at each frequency (not simultaneously). This forms 2 independent load cases which, when used together, completely determines all 4 complex Z's at each test frequency.

$$\begin{bmatrix} \bar{x}_f & \bar{y}_f & 0 & 0 \\ 0 & 0 & \bar{x}_f & \bar{y}_f \\ \bar{x}_b & \bar{y}_b & 0 & 0 \\ 0 & 0 & \bar{x}_b & \bar{y}_b \end{bmatrix} \begin{Bmatrix} Z_{xx} \\ Z_{xy} \\ Z_{yx} \\ Z_{yy} \end{Bmatrix} = \begin{Bmatrix} \bar{F}_{xf} \\ \bar{F}_{yf} \\ \bar{F}_{xb} \\ \bar{F}_{yb} \end{Bmatrix} \qquad \begin{matrix} f = forward \\ b = backward \end{matrix} \tag{4}$$

The 8 components are plotted versus frequency, and curve fits yield the desired rotordynamic coefficients which can now all be complex. This test approach was used by Kanki, et al. (ref. 3). Note that it is better to combine the forward and backward data to completely determine the Z's over the frequency range from f_{low} to f_{high}, rather than keeping them separate and using equation (3) to partially determine the Z's from $-f_{high}$ to $+f_{high}$ (see Ohashi, et al. (ref. 4) and Jery, et al. (ref. 5)). This same conclusion was also reached by Bolleter, et al. (ref. 6). Note also that forward and backward circular orbits taking place at the same time form an ellipse, but a single ellipse is a single load case and does not completely determine the Z's (see below).

The technique of actually plotting and inspecting the impedance functions versus frequency, followed by a curve fit, provides insight into the mechanisms at work, and also experimental scatter. The importance of this visualization apparently has been overlooked by some researchers. As opposed to plotting and curve fitting the impedance functions, the force and displacement data for some or all frequencies can be assembled into a single matrix equation as follows (i.e., rearrangement of the terms of equation (2a)):

$$\begin{aligned} [displacement\ data\ matrix]\{KCM\ vector\} &= \{force\ data\} \\ [4 * \#\ frequencies\ by\ 12]\{12\ by\ 1\} &= \{4 * \#\ frequencies\ by\ 1\} \end{aligned} \tag{5}$$

The 12 rotordynamic coefficients can be real or complex and are computed directly by either using a subset of the data to write exactly 12 equations (Adams, et al. (ref. 2)), or using all the data and performing a least squares solution (Nordman, et al. (ref. 7), Goodwin, et al. (ref. 8), and Burrows, et al. (ref. 9)). The latter approach will produce rotordynamic coefficients identical to those produced by plotting and curve fitting, but without the benefit of seeing this graphically.

Another approach to bypassing the impedance functions and proceeding directly to 12 unknown rotordynamic coefficients is to use a recursive estimation scheme on time domain data (Stanway (ref. 10), Sahinkaya, et al. (ref. 11), and Ellis, et al. (ref. 12)). This should yield a result similar, if not identical, to the frequency domain approach of equation (5). Among its advantages are; transformation to the frequency domain with its associated windowing functions is not needed, rotordynamic coefficients can conceivably be computed on-line during test (i.e., like a filter), and it is an effective way to deal with time varying parameters (Goodwin and Payne (ref. 13)). Again, however, there is will be no graphical check on the validity of the KCM model.

Single Elliptic Orbit - The magnetic bearing can also be used to impart elliptic motion to the rotor, and vary its frequency over the frequency range of interest (rotor speed held constant). Data for a single elliptic orbit contains the same amount of information as a single circular orbit, but must be utilized differently because of its different form. For example, to use the technique of equation (3), $\bar{y}/\bar{x}$ must be constant. The displacement orbit must have a constant ratio of major to minor axis length, and must have constant orientation. It is probably not practical to satisfy these conditions. Instead, the approach of equation (5) could be used to directly compute 12 real rotordynamic coefficients. In this case it is desirable that the displacement ellipse be highly variable as a function of frequency to get the best definition of the rotordynamic coefficients. In fact, the further removed from a circle the data becomes, the more important it is that the ellipses be highly varied. It can be shown that the limiting case of a constant, purely translational orbit would render the matrix of equation (5) singular. When solving the least squares form of equation (5) it is best to use a Singular Value Decomposition (SVD) algorithm (Forsythe, et al. (ref. 14)) to get a direct indication of the quality of the solution (i.e., the matrix condition number). One can also use the statistical parameters employed by Burrows, et al. (ref. 9) to help quantify the accuracy of the least squares solution. It is interesting to note that some simple numerical experiments on equation (5) have shown that varied elliptic data can easily yield a solution twice as good as circular data. In exchange for the more precise solution, however, it is no longer possible to plot impedance functions versus frequency to provide a visual check of the validity of the KCM model.

Another approach to utilizing data for one ellipse per frequency is to assume the impedances to be skew symmetric (i.e., $Z_{xx} = Z_{yy}$ and $Z_{xy} = -Z_{yx}$). In this case equation (2b) becomes (see Bolleter, et al. (ref. 6)):

$$\begin{bmatrix} 1 & \bar{a} \\ -\bar{a} & -1 \end{bmatrix} \begin{Bmatrix} Z_{xx} \\ Z_{xy} \end{Bmatrix} = \begin{Bmatrix} \bar{F}_x/\bar{x} \\ \bar{F}_y/\bar{x} \end{Bmatrix} \qquad \bar{a} = \frac{\bar{y}}{\bar{x}} \tag{6}$$

As long as $\bar{a}$ is not $\pm i$ (i.e., not a circle), the two complex impedances can be computed using Cramer's rule, and plotted versus frequency. The plots provide a check on the KCM model, and curve fits yield 6 complex rotordynamic coefficients (K_{xx}, C_{xx}, M_{xx} and K_{xy}, C_{xy}, M_{xy}). The coefficients would be expected to be real, but need not be. For example Bolleter, et al. (ref. 6) detected hysteretic damping (complex K_{xx}) in boiler feed pump impellers using this approach. Note that the orbit must be elliptic. As $\bar{a}$ approaches $\pm i$ the solution for Z_{xx} and Z_{xy} becomes ill-defined, and is undefined when $\bar{a} = \pm i$. The following expression is an amplification factor for uncertainties in both $\bar{x}$ and $\bar{y}$:

$$f = \frac{1}{2(|a| - 1)} \tag{7}$$

If there is 5% uncertainty in $\bar{x}$ then there is f*5% uncertainty in Z_{xx} and Z_{xy}. The need to avoid circles in this case is apparent. One other potential drawback of assuming skew symmetric impedances is what happens when this assumption is violated. For example, if K_{xx} equals 90% of K_{yy} this could manifest itself as a bias in K_{xy}, or produce seemingly significant amounts of C_{xy} when in fact there is none.

Dual Elliptic Orbits- The magnetic bearing could be used to produce two different elliptic orbits at each test frequency (not at the same time). This forms two independent load cases, and is analogous to the case of forward and backward circles described earlier. In fact, the forward and backward circles is a special case of 2 ellipses. When using two ellipses it is imperative that they be independent so that the 4 Z's can be computed employing equation (4) for each frequency. The condition number (Forsythe, et al. (ref. 14)) of the matrix in equation (4) quantifies the degree of independence. The following expression due to Zhang, et al. (ref. 15) can be used to calculate the condition number at each frequency:

$$COND = \frac{B + \sqrt{B^2 - 4|\bar{x}_2\bar{y}_1 - \bar{y}_2\bar{x}_1|}}{B - \sqrt{B^2 - 4|\bar{x}_2\bar{y}_1 - \bar{y}_2\bar{x}_1|}} \tag{8}$$

where $B = |\bar{x}_1| + |\bar{x}_2| + |\bar{y}_1| + |\bar{y}_2|$. The condition number is similar to f of equation (7), and in this case is an upper limit on amplification of error. The minimum, or optimum, value is 1 which occurs only with orthogonal translational orbits of equal amplitudes. The maximum value is infinite which occurs with identical orbits (can have different sizes). A pair of forward and backward circular orbits of equal radius yields a condition number of 5.83. Adequate solutions to equation (4) can be plotted versus frequency for subsequent inspection and curve fitting. Excessive condition numbers will make the impedance curves appear "noisy" regardless of the actual signal/noise ratios. This latter fact is easily overlooked. When the condition numbers are too high one must resort to the techniques for single elliptic data. Numerical experiments presented by Zhang, et al. (ref. 15) dictate that a practical cutoff on condition number may be about 20 to 30.

It has been suggested that the 4 stiffness and 4 damping values (no inertia) can be obtained solely from unbalance response data at a single speed (Lund (ref. 16), Zhang, et al. (ref. 15), Lee, et al. (ref. 17) and related paper by Verhoeven (ref. 18)). This fits the two ellipse case for a single frequency. Either two identical bearings on one shaft must experience different elliptic orbits simultaneously under the action of a single unbalance distribution, or one bearing must experience different ellipses at the same speed under two different unbalance distributions. Either case can apparently be achieved in practice with a carefully designed experiment. The degree of success will depend not only on the accuracy of the bearing displacements and forces, but also on the value of the condition number of equation (8).

CURRENT TEST APPROACH

In light of the preceding discussion, it has been decided that, if possible, a test approach would be used which enables plotting of impedance functions versus frequency without assuming skew symmetry. This implies either the single circular orbit approach, or dual elliptic orbit approach. The dual elliptic approach is preferable as it completely determines the impedance functions, but may require twice the test time as the single circular approach. As mentioned earlier the length of test time is severely limited. So arbitrarily large numbers of samples will not be available for averaging out system noise. As a first step we will attempt to achieve purely translational rotor motion first in one axis and then the other. This would provide the most accurate impedance determination possible according to equation (8). The system may, however, prove to be too noisy such that there is not ample time to get enough averages when executing the two load cases sequentially. Burrows, et al. (ref. 9) and Yasuda, et al. (ref. 19) applied their load cases simultaneously via alternating harmonics and statistical independence, respectively. If necessary, we will try the method of Burrows, but at this time it is unclear whether these are viable ways to overcome a problem of insufficient averaging time. If the impedance measurements still suffer from excessive noise, we will resort to the single circular orbit approach. Should it happen that the magnetic bearing cannot satisfactorily enforce a circular orbit, we shall use the method of single elliptic data. Depending on the overall success, or lack thereof, of the current test program, future testing may employ recursive time domain methods mentioned earlier.

EXCITATION SIGNAL

The radial magnetic bearing serves as a non-contacting, dual-axis electrodynamic shaker. Its power supply has an input jack for each axis such that it can perform as 2 independent shakers. In actuality the magnetic bearing system is unproven in this regard, and at this time it still remains to be seen how well it will perform this function. Our goal is to measure the transfer functions of bearing force to bearing displacement. Since test time is at a premium, the input signal should provide a good combination of accuracy and rapidity. Another consideration is the frequency range of interest will span up to 4 system resonances which will be functions of pressure drop, shaft rpm, etc. The magnetic bearing system itself also has highly nonlinear frequency response characteristics (Hawkins, et al. (ref. 1)). It is desirable that the input signal can be spectrally shaped in an adaptive fashion so a flat displacement spectrum can be achieved on output. This will enable higher signal to noise ratios over the entire frequency range without overloading the system at the resonances. A flat displacement spectrum also makes it easier to investigate amplitude dependent nonlinearities by driving the system to progressively higher response levels.

Single frequency steady state sinusoidal testing is unquestionably the best way to fit a linear model to a real system (Herlufsen (ref. 20)), but the long test time precludes its use here. Fortunately, work by Bolleter, et al. (ref. 6), Yasuda, et al. (ref. 19) and Chang, et al. (ref. 21) indicate that a multifrequency input signal gives virtually identical results as single frequency testing. Yasuda's testing was steady state as they used random input signals. Bolleter's testing was transient as he used a rapid sine sweep, or chirp. Chang's testing was also transient as he used impact. The article by Herlufsen (ref. 20)

discusses some of the aspects, and different types, of steady state and transient testing. Since we intend to modify the input signal during test in an adaptive fashion to achieve a flat displacement spectrum, a transient signal is the logical choice.

Step (Morton (ref. 22)), impulse (Nordman, et al. (ref. 7)) and chirp (Bolleter, et al. (ref. 6)) are examples of transient input signals. Bolleter obtained excellent results using a chirp input. Also, the spectrum of a chirp can be easily shaped to virtually any desired form. Papers by White, et al. (ref. 23) and White (ref. 24) provide the technical aspects of using a chirp input signal. The chirp is thus our chosen input signal (see figure 2). Our test approach will be to input a series of chirps along one axis including the modification of each successive chirp to converge on a flat displacement spectrum. This is then repeated along the other axis. Very elongated elliptic orbits should result as long as the rotordynamic cross-coupling is not too strong. This data will then be used with the dual elliptic reduction method described earlier.

DATA ACQUISITION AND PROCESSING

A digital computer will be used to sample, and store on-line, all data channels necessary to produce rotordynamic coefficients. Prior to testing, a common broadband random signal will be input simultaneously to all channels of the data acquisition system. Interchannel transfer functions thus obtained will be used as correction factors to match the gain and phase of all channels, including filters. The same computer system will be used to compute and output the chirp signals. The computer system is capable of performing an on-line spectral analysis of the displacement response, and modifying each successive chirp accordingly.

The complex quantities $\bar{x}$, $\bar{y}$, $\bar{F}_x$ and $\bar{F}_y$ are needed for equation (4) so that the impedances can be calculated. The effects of system noise can be more effectively reduced if one works with transfer functions computed from spectral densities (see Bendat, et al. (ref. 25) or Halvorsen, et al. (ref. 26)). Thus in practice the computer will be used to compute cross and auto spectral densities from each series of chirps. These are used to compute transfer functions $\bar{F}_x/\bar{x}$, $\bar{F}_x/\bar{y}$, $\bar{F}_y/\bar{x}$ and $\bar{F}_y/\bar{y}$ as functions of frequency. For each frequency these 8 complex values (4 from the x chirps and 4 from the y chirps) are used with equation (4) to compute the complex impedances, Z. All calculations are to be done post-test by the same computer used for acquisition. Hard copy plots of the impedance functions, along with curve fits for rotordynamic coefficients, are the end product of each test.

SUMMARY

A multifunction test apparatus has been described which will be used to measure rotordynamic coefficients of bearings and seals. A radial magnetic bearing will be used to load the shaft statically and excite dynamic motion of the rotor in a controlled fashion which will enable complete definition of the test element's rotordynamic impedances as functions of frequency. Transient testing will be performed with chirp input signals being applied separately to the inertial x and y axes of the rotor. The chirp input signals will be modified on-line to achieve flat displacement spectrums at the test element. The test approach and the data reduction methodology were described in detail. The testing environment closely matches real rocket engine turbopump operating conditions in speed, pressure, clearance,

temperature, working fluid, etc. Overall, this is considered a very ambitious test program, technically. Initial testing is currently expected to take place in the summer of 1990.

NOMENCLATURE

$\bar{a}$	$\bar{y}/\bar{x}$
B	$\lvert\bar{x}_1\rvert + \lvert\bar{x}_2\rvert + \lvert\bar{y}_1\rvert + \lvert\bar{y}_2\rvert$
COND	matrix condition number
F	$\{F_x, F_y\}^T$
F_x, F_y	real test element force
$\bar{F}_x, \bar{F}_y$	complex test element force
f_{low}, f_{high}	limits of test frequency range
f	error amplification factor
K	test element stiffness matrix
C	test element damping matrix
M	test element inertia matrix
KCM	stiffness, damping and inertia
q	$\{x, y\}^T$
x,y	real displacements of test element
$\bar{x}, \bar{y}$	complex displacements of test element
Z	complex impedance of test element
i	$\sqrt{-1}$
ω	frequency of harmonic motion (rad/sec)
$\lvert\bar{x}\rvert$	magnitude of complex number $\bar{x}$

REFERENCES

1. Hawkins, L., Murphy, B. and Lang, K., "The Rocketdyne Mutlifunction Tester - Part II: Operation of a Radial Magnetic Bearing as an Excitation Source," Workshop on Rotordynamic Instability Problems in High Performance Turbomachinery, Texas A&M University, May, 1990.

2. Adams, M., Makay, E. and Diaz-Tous, I., "Measurement of Interstage Fluid-Annulus Dynamical Properties," Workshop on Rotordynamic Instability Problems in High Performance Turbomachinery, Texas A&M University, NASA CP2250, May, 1982, pp. 147-156.

3. Kanki, H. and Kawakami, T., "Experimental Study on the Static and Dynamic Characteristics of Screw Grooved Seals," ASME Publication DE-Vol. 2, *Rotating Machinery Dynamics*, Volume 1, Sept., 1987, pp. 273-278.

4. Ohashi, H. and Shoji, H., "Lateral Fluid Forces Acting on a Whirling Centrifugal Impeller in Vaneless and Vaned Diffuser," Workshop on Rotordynamic Instability Problems in High Performance Turbomachinery, Texas A&M University, NASA CP2338, May, 1984, pp. 109-122.

5. Jery, B., Acosta, A., Brennan, C. and Caughey, T., "Hydrodynamic Impeller Stiffness, Damping and Inertia in the Rotordynamics of Centrifugal Pumps," Workshop on Rotordynamic Instability Problems in High Performance Turbomachinery, Texas A&M University, NASA Conference Publication 2338, May, 1984, pp. 137- 160.

6. Bolleter, U. and Wyss, A., "Measurement of Hydrodynamic Interaction Matrices of Boiler Feed Pump Impellers," ASME Paper No. 85-DET-148, Sept., 1985.

7. Nordmann, R. and Massmann, H.,"Identification of Dynamic Coefficients of Annular Turbulent Seals," Workshop on Rotordynamic Instability Problems in High Performance Turbomachinery, Texas A&M University, NASA CP2338, May, 1984, pp. 295-311.

8. Goodwin, M. J., Penny, J. E. T. and Hooke, C. J., "Hydrostatic Supports for Rotating Machinery - Some Aspects of Oil Film Non-Linearity," ASME Paper No. 85-DET-123, Sept., 1985.

9. Burrows, C., Kucuk, N., Sahinkaya, M. and Stanway, R., "Estimation of Squeeze-Film Bearing Inertia, Damping and Stiffness Coefficients," ASME Publication DE-Vol. 2,*Rotating Machinery Dynamics*, Volume 1, Sept., 1987, pp. 109-114.

10. Stanway, R., "Journal Bearing Identification Under Operating Conditions," ASME Journal of Dynamic Systems, Measurement and Control, Vol. 106, 1984, pp. 178-182.

11. Sahinkaya, M. and Burrows, C., "Kalman Filters Applied to Time-Domain Estimation of Linearized Oil-Film Coefficients," I. Mech. E. Conference Publication 1984-10, Vibrations in Rotating Machinery, 1984, pp.109-118.

12. Ellis, J., Roberts, J. and Hosseini Sianaki, A., "A Comparison of Identification Methods for Estimating Squeeze-Film Damping Coefficients," ASME Journal of Tribology, Vol. 110, Jan., 1988, pp. 119-127.

13. Goodwin, G. and Payne, L., *Dynamic System Identification*, Academic Press, London, 1977.

14. Forsythe, G., Malcolm, M. and Moler, C., *Computer Methods for Mathematical Computations*, Prentice Hall, Englewood Cliff, New Jersey, 1977.

15. Zhang, Q., Lallement, G. and Fillod, R., "Identification of the Dynamic Characteristics of Oil Film Bearings," ASME Publication DE-Vol. 2, *Rotating Machinery Dynamics*, Volume 1, Sept., 1987, pp. 57-61.

16. Lund, J., "Evaluation of Stiffness and Damping Coefficients for Fluid-Film Bearings," *The Shock and Vibration Digest*, Vol. 11, No. 1, Jan., 1979, pp. 5-10.

17. Lee, C. and Hong, S., "Identification of Bearing Dynamic Coefficients by Unbalance Response Measurements," I. Mech. E., Part C, Vol. 203, 1989, pp. 93-101.

18. Verhoeven, J., "Excitation Force Identification of Rotating Machines Using Operational Rotor/Stator Amplitude Data and Analytical Synthesized Transfer Functions," ASME Publication DE-Vol. 2, *Rotating Machinery Dynamics*, Volume 1, Sept., 1987, pp. 207-214.

19. Yasuda, C., Kanki, H., Ozawa, Y. and Kawakami, T., "Application of Random Excitation Technique to Dynamic Characteristic Measurement of Bearing," Proceedings of the JSME, 1986, pp. 61-67.

20. Herlufsen, H., "Dual Channel FFT Analysis (Part I)," Bruel-Kjaer Technical Review No. 1-1984, 1984.

21. Chang, K., Chong, F. and Rowe, W., "Journal Bearing Vibration - a Comparison of Sinusoidal Excitation with Impact Excitation," *Proceedings of the 1st European Sponsored Turbomachinery Conference*, SAE No. 864965, 1986, pp. 83-89.

22. Morton, P., "The Derivation of Bearing Characteristics by Means of Transient Excitation Applied Directly to a Rotating Shaft," *Dynamics of Rotors*, Springer-Verlag, New York, 1975.

23. White, R. and Pinnington, R., "Practical Application of the Rapid Frequency Sweep Technique for Structural Frequency Response Measurement," *Aeronautical Journal*, May, 1982, pp. 179-198.

24. White, R., "Spectrally Shaped Transient Forcing Function for Frequency Response Testing," *Journal of Sound and Vibration*, 23(3), 1972, pp. 307-318.

25. Bendat, J. and Piersol, A., *Engineering Applications of Correlation and Spectral Analysis*, John Wiley and Sons, New York, 1980.

26. Halvorsen, W. and Brown, D., "Impulse Technique for Structural Frequency Response Testing," *Sound and Vibration Magazine*, Nov., 1977, pp. 8-21.

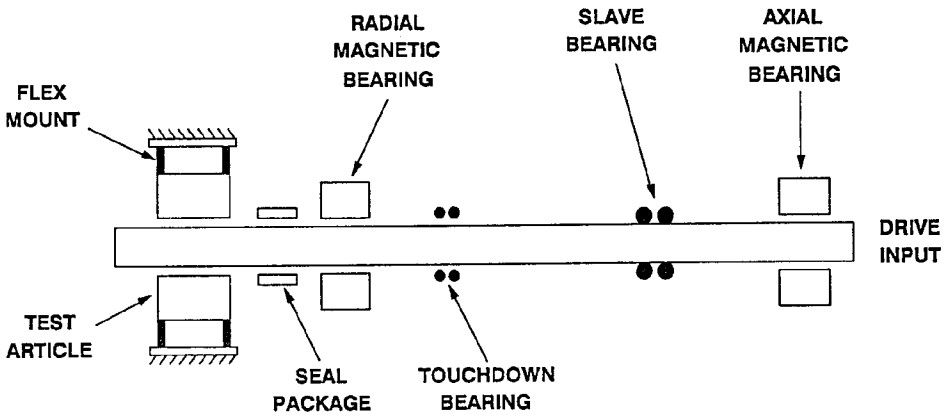

FIGURE 1) Schematic of mutlifunction tester.

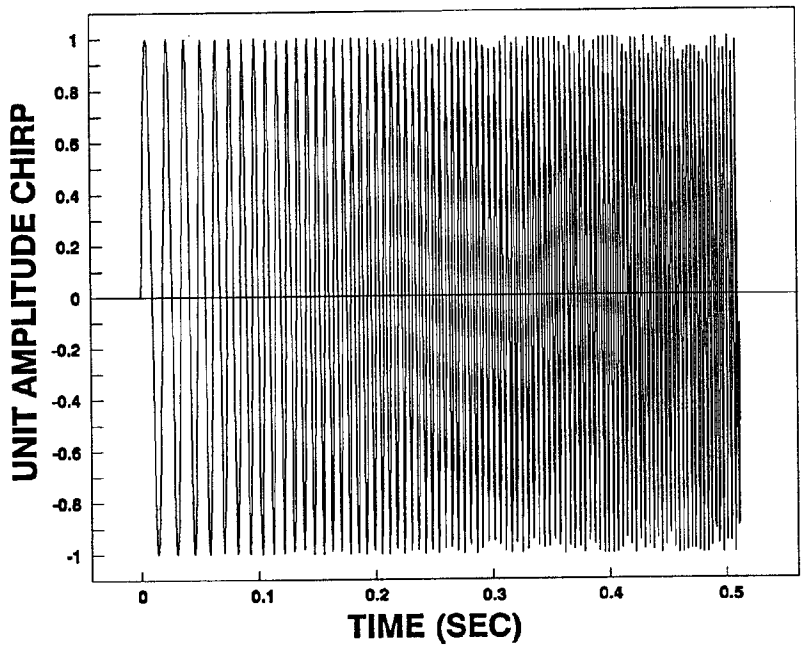

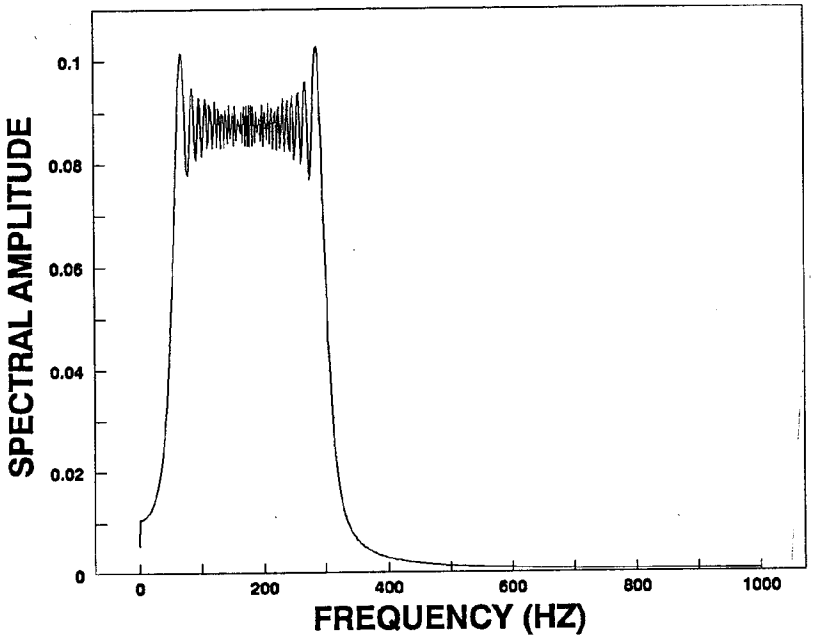

FIGURE 2a) unit amplitude chirp, 50-350 Hz in 0.512 seconds, 2000 Hz sample rate. FIGURE 2b) amplitude spectrum of a).